Chapter 9
Risk and Exposure to Extreme Heat in Microclimates of Phoenix, AZ

Darren M. Ruddell, Sharon L. Harlan, Susanne Grossman-Clarke, and Alexander Buyantuyev

Abstract As rapid urban development continues, the impacts of temperature extremes on human health and comfort are expected to increase as threshold temperatures of human tolerance are crossed more frequently and for longer periods of time. This study examined extreme heat as an urban hazard throughout the Phoenix (Arizona, USA) metropolitan area during a four-day 2005 summer heat wave. Utilizing the Weather Research and Forecasting (WRF) model to simulate 2 m air temperature variability throughout the region, the distribution of threshold temperatures and heat exposure was examined in 40 diverse neighborhoods. Neighborhood residents also responded to a social survey about perceived temperatures and heat-related health problems during the summer of 2005.

  Results indicated that extreme heat was variably distributed throughout the neighborhoods; residents' perceptions of temperature and self-reported experiences with heat-related illnesses were related to environmental conditions; the highest risk of exposure to extreme heat was among elderly, minority, and low-income residents; and land use/cover characteristics exhibited strong relationships with local threshold temperatures. Research contributions include the development of a geotechnical analysis method that could help cities to prepare for and respond to the most vulnerable residents during periods of extreme heat as well as the interrelation of regional atmospheric model results with socio-economic data.

Keywords Climate · Hazard · GIS · Environmental justice · Urban heat island · Weather-forecasting

9.1 Introduction

Cities in most types of climate regimes are becoming warmer over time and, consequently, urban populations are increasingly vulnerable to the hazards of summertime heat. In cities, the effect of rising global temperatures is compounded by regional

D.M. Ruddell (✉)
School of Geographical Sciences, Arizona State University, Tempe, AZ 85287-0104, USA
e-mail: darren.ruddell@asu.edu

climate change caused by large-scale, rapid urbanization. The global average temperature has risen 0.5°C since the 1970s (McMichael et al. 2006) but in roughly the same period, differences between temperatures in the city compared to surrounding rural areas have been measured ranging from 1 to 12°C (Aniello et al. 1995; Brazel et al. 2000; Voogt 2002). One study found that US cities, on average, experience 10 more hot summer nights than they did 40 years ago (DeGaetano and Allen 2002).

Urbanization affects physical processes that alter the surface energy balance, and therefore, near-surface air temperatures (Arnfield 2003; Oke 1982). For example, surface cooling is inhibited by reduced outgoing long-wave thermal radiation due to the vertical structure of buildings, and sources of anthropogenic heat (e.g., vehicles, air conditioners, and industry) exhaust heat into the air near the urban surface (Grossman-Clarke et al. 2005). High heat capacity and thermal conductivity of building materials lead to greater storage of heat in the city compared to the natural land covers and agricultural land uses that preceded urbanization. These changes produce what has been described as the urban heat island (UHI) effect, where cities experience higher nighttime temperatures and generally higher but more variable daytime temperatures than the surrounding less built-up areas (Lowry 1967; Oke 1997; Voogt 2002). However, data acquired through remote sensing, surface weather stations, and regional atmospheric modeling also indicate significant temperature variability within urban areas (Arnfield 2003; Voogt and Oke 2003; Grimmond 2005). It is likely that urban vegetation serves as a mitigating factor against warm temperatures for some areas of the city while exacerbating high temperatures for other areas (Stabler et al. 2005; Jenerette et al. 2007). Much of the intra-urban temperature variation is, therefore, driven by human decisions and resources that determine residential land use/land cover (LULC) within the urbanized region.

Not only are cities experiencing chronic temperature increases, but global warming and UHIs are jointly responsible for causing more extreme heat events in cities. Extreme (acute) heat events, defined as sustained high temperatures exceeding the normal range of temperature variability, occur throughout the world and are projected to become more intense, more frequent and longer lasting over the next century (IPCC 2007; Meehl and Tebaldi 2004).

There is ample evidence that prolonged exposure to excessively warm weather is a major human health hazard, especially at junctures when critical temperature thresholds in cities are abruptly crossed (Sheridan and Kalkstein 2004). Temperature-mortality relationships are evident in temperate as well as warmer climate regimes (Patz et al. 2005). More people die in the US from extreme heat than any other weather-related phenomenon (CDC 2006) and very hot weather increases mortality rates as well as hospital admissions for cardiovascular, respiratory, and other pre-existing illnesses (Semenza et al. 1999). The 1995 Chicago heat wave, for instance, claimed over 700 lives (Semenza et al. 1996). Between 22,000 and 52,000 Europeans died during the 2003 heat wave, many of them in large cities (Larson 2006). Less publicized cases of heat waves in India and other Asian cities also report high excess death rates (e.g., Choi et al. 2005). As rapid

urban development continues, the impacts of heat-related hazards on human health and comfort are also expected to increase as the threshold of human tolerance to rising temperatures are crossed more frequently and for longer periods of time (Kalkstein and Greene 1997). The Intergovernmental Panel on Climate Change (IPCC) projects with "medium confidence" a future increase in heat wave-related deaths worldwide (Confalonieri et al. 2007). The number of heat-related fatalities could double in the near future (Larson 2006 citing the World Meteorological Association).

Almost all epidemiological studies treat the city as a single entity in tallying the temperature-related mortality during and immediately after heat events (Braga et al. 2002; Curriero et al. 2002; Michelozzi et al. 2006; Smoyer et al. 2000). Recently, heat watch-warning systems have been developed to mitigate the health impacts of sudden heat events by providing advance notification of dangerously warm weather. The warning systems are sensitive to local synoptic weather variables that vary from city to city, but they rely on data from a single, centrally-located weather station in each city and the warnings are broadly applied to entire urban areas (Sheridan and Kalkstein 2004; Smoyer-Tomic and Rainham 2001). Thus, current heat watch-warning systems lack sensitivity to intra-urban microclimate variation and the precise locations where heat hazards are the greatest.

Heat-health studies often find that advanced age and some types of chronic illnesses and disabilities are associated with higher morbidity rates attributable to extremely hot weather (McGeehin and Mirabelli 2001; Kilbourne 2002). These variables are treated as individual characteristics that predispose people to physiological weaknesses which, in turn, increase their vulnerability to heat. Other high risk populations, such as racial minorities and people living in poverty, often have poorer general health and lack access to air conditioning and critical socioeconomic resources (O'Neill et al. 2003; Naughton et al. 2002). Klinenberg's (2002) study of the 1995 Chicago heat wave disaster found that deaths among the elderly were most numerous in a few neighborhoods with high concentrations of minority residents who lacked strong social networks and support systems. The associations between characteristics of urban residents and risk of heat-related health problems can also be caused by environmental conditions in the places where they live. In one study, affluent whites lived in neighborhoods that were several degrees cooler in the summer of 2003 than low-income and Latinos neighborhoods (Harlan et al. 2006, 2008; Jenerette et al. 2007). Residents in the warmest neighborhoods spent 20% of the entire summer in conditions that exceeded the "danger" threshold on a heat stress index.

9.2 The Study

One of the most effective ways to reduce the impacts of disasters that cause large scale environmental health problems is to obtain "accurate exposure assessments" (Patz 2005). Recent advances in the accuracy, resolution, and sensitivity of geospatial tools and weather simulation models have enhanced our ability to

identify the locations of the places and people that are most vulnerable to extreme heat within cities.

This study examined the spatial distribution of air temperature during an extreme heat event and the exposure of people to threshold temperatures (defined in Section 2.2.1) at a very fine spatial resolution in the Phoenix (Arizona, USA) metropolitan area. By means of combining remote sensing and GIS techniques, regional atmospheric modeling, and socioeconomic data, we developed a geospatial tool to analyze heat hazards for Phoenix. We applied the Weather Research and Forecasting (WRF) model developed by the National Center for Atmospheric Research (Shamrock et al. 2005) to simulate 2 m air temperatures in the Phoenix metropolitan area during a four-day heat event in July 2005 and subsequently to quantify the heat hazard by hours of human exposure to threshold air temperatures for 40 diverse neighborhoods throughout the urban region. The model showed marked contrasts in temperature across neighborhoods.

Social survey data on residents' perceptions of temperature and experiences with illnesses caused by heat stress were related to the results of the weather simulation model. To assess human risk, WRF model output was compared to US Census block group population characteristics, which showed how exposure to extreme temperature varied by socioeconomic status (household income), ethnicity, and age composition of the neighborhood. As far as we are aware this was the first time that socioeconomic data have been interrelated with output from a regional atmospheric model. Finally, the association of air temperature with LULC was examined to better understand the mitigating influence of landscapes on local microclimate variability.

The variable temperatures and landscapes within the Phoenix UHI create a thermal "riskscape" of heat hazards that are distributed unevenly over the city and impact people differently. During a period of elevated temperature (i.e., heat wave), the places inhabited by populations that were least likely to have key economic and natural resources were more exposed to hazardous conditions. This study provides information that may help to prevent health disasters related to extreme heat in cities by answering three important research questions: *(1) How are heat hazards distributed among places in the Phoenix metropolitan area? (2) How closely do residents' perceptions of temperature and experience with heat-related illnesses align with simulated air temperatures in their neighborhoods? (3) Within the study area, what types of residents were most at risk and can certain types of local landscape serve as mitigating influences on temperature?*

9.2.1 Research Methods

For the investigation of heat-related hazards in urban areas there is clearly a need to better understand the distribution of air temperatures in relation to residents' means to cope with extreme heat within a regional study area. Using a multi-method approach, we examine data on threshold temperatures, analyze the spatial distribution of the data, and interpret the results.

9.2.2 Study Area

Located in the Sonoran Desert of the southwestern United States, the Phoenix metropolitan area is an ideal setting for studying human vulnerability to high temperatures (Fig. 9.1). Encompassing over 1800 square miles in Central Arizona, metropolitan Phoenix is home to over 65% of the state's 6.1 million residents (Census Bureau 2006). The city has a naturally warm climate and over the past 50 years of population growth, the average daily temperature has increased by more than 3°C (Brazel et al. 2000). The 2005 summer season which began June 21st and ended September 22nd, witnessed record (16 records tied or broken) high temperatures in the day as well as the evening. The Center for Disease Control (CDC 2005) recently reported that Arizona led the nation in heat-related deaths from 1993–2002. Although Phoenix has experienced a steady rise in average daily temperature, human exposure to high temperatures varies widely throughout this region. For example, Hedquist and Brazel (2004) measured average nighttime maximum temperature variation on a rural to urban gradient equal to 7.3°C in 2001.

Within the metropolitan area, the present study concentrates on 40 diverse neighborhoods under study as part of the 2006 Phoenix Area Social Survey (PASS) project. These neighborhoods offer insight into the spatial distribution of temperature variability throughout the region during a summer heat event, in addition
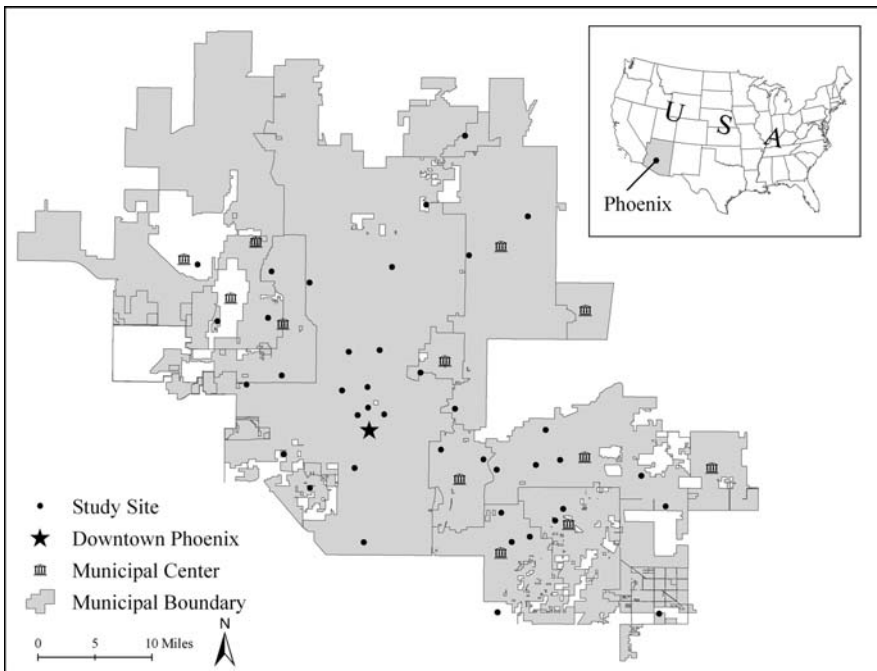

Fig. 9.1 Map of metropolitan Phoenix, Arizona

to a survey of residents' perceptions of and experiences with extreme heat. PASS employed a two-stage research design (Harlan et al. 2007). First, a systematic sample of 40 neighborhoods was selected from the 94 urban sites that are monitored by the Central Arizona-Project Long-Term Ecological Research CAP LTER project (Grimm and Redman 2004). Census data by block group were assembled for all 94 sites and classified by location (urban core, suburban, and fringe), median income, and ethnic composition. All types of neighborhoods in the Phoenix area were represented among the sample of 40. Second, a random sample of households within each neighborhood was selected to participate in a social survey, which is described in more detail below.

9.2.3 Extreme Heat Event Period

Following criteria used by Meehl and Tebaldi (2004), periods of extreme heat were identified in a three-step process. The first step was to examine National Oceanic and Atmospheric Administration (NOAA) temperature readings for Phoenix, AZ's Sky Harbor International Airport weather station, which is commonly used in climate studies (Brazel et al. 2000). This data set was used to determine normal historical (1961–1990) temperature variability in comparison to present day (2005) conditions. Second, using observed temperature readings, we calculated the distribution in percentiles for normal and present day summer temperatures. The third and final step to identify period(s) of extreme heat for the summer of 2005 was to compare the normal and present day conditions based on the three criteria of threshold temperatures (Threshold 1 [T1]: the 97.5 percentile of the observed distribution; and T2: the 81 percentile) identified by Meehl and Tebaldi (2004). Temporal periods satisfying all three of the following conditions are considered to be extreme heat events: (1) daily maximum temperature must be above T1 for at least three days; (2) average daily maximum temperature must be above T1 for the entire period; and (3) daily maximum temperature must be above T2 for the entire period.

After completing this process, the local threshold temperatures, based on normal conditions, were: T1 = 45°C (113°F); and T2 = 42°C (108°F). Comparing 2005 temperatures readings to normal conditions, there were three distinct heat events in the Phoenix metropolitan area on June 6–9; July 15–19; and August 1–3. The temporal period examined in this study is the four-day heat event from July 15–19, 2005, which represents the longest and most intense heat event during the year. The WRF model, described in the next section, was applied to simulate 2 m air temperature variability and exposure to threshold temperatures throughout the 40 neighborhoods.

9.2.4 WRF Modeling of Heat Event

An important step in the analysis of heat hazards in relation to human exposure is quantifying air temperature, usually at a height of 2 m, at appropriate spatial and

temporal scales. The spatial variability of temperatures in urban regions is more complex than a linear gradient from urban core to fringe, and an emerging theme of research on urban climate is to determine the factors that are associated with temperature variation. Current techniques to quantify air temperatures include measurements from weather stations and spatial information tools such as remote sensing or atmospheric models that simulate air temperature. Existing methods to quantify air temperature all possess various strengths and weaknesses. Surface meteorological stations, for example, offer precise information on air temperature changes over time at discrete sites in the urban area, but usually lack dense spatial coverage. Alternatively, remote sensing provides detailed spatially and temporally consistent information on surface temperature variability within urban areas, but it is limited to discrete temporal "snapshots" and surface temperatures are not necessarily an indicator of the magnitude of air temperature.

Modeling and simulation techniques continue to gain traction within the scientific community by offering new ways to study interactions of physical and social processes in urban areas where most humans live. The term model, as used in the context of meteorology and climate, refers to a complex computer code that numerically solves a set of differential equations that govern the evolution of the state of the atmosphere in space and time in terms of air temperature, pressure, specific humidity and wind speed. The evolution is determined in part through the interaction between the model variables, but also through external forcing (e.g. solar radiation) and interactions with the earth's surface through fluxes of heat, moisture and momentum. Physical properties of the earth's surface that influence the exchange with the atmosphere depend on land use/cover characteristics. The accurate characterization of LULC and corresponding physical properties therefore is an important input variable for meteorological models. The output of a global atmospheric model together with observations of the atmosphere are generally used to quantify initial and boundary conditions for the fine resolution regional model to determine atmospheric features that cannot be captured by the physical processes included in the regional model. Other methods for determining air temperature within urban areas are limited by the accuracy of regional atmospheric models that depend, among other factors, on limited knowledge of physical processes in the atmosphere and their mathematical description, as well as uncertainties in initial and boundary conditions as supplied by the global model.

Relatively recent developments in geocomputation have enabled advances in regional atmospheric models to resolve heterogeneity within urban areas, which, in turn, have inspired the development of model approaches that describe the energy exchange between the urban surface and the atmosphere by the climate community (Brown 2000; Masson 2006; Martilli 2007). The application of such schemes within atmospheric models have greatly improved the accuracy of urban air temperature simulations over the past 10 years, and today such models are widely employed to enhance scientific understanding of processes related to neighborhood scale climate and air quality (Taha 1997a, b; Civerolo et al. 2000; Seaman 2000; Lin et al. 2008).

This study combined WRF version 2 (Shamrock et al. 2005) together with the urban surface energy balance model by Kusaka and Kimura (2004) to simulate

2 m air temperatures for the period July 15–19, 2005. The model's spatial resolution of 1 km for horizontal model grid cells corresponds well with neighborhood block group data obtained from the Census. Since the average urban block group is about $\frac{1}{4}$ square mile, the model's spatial resolution of 1 km (or 0.39 square miles) roughly covers the same area. Grossman-Clarke et al. (2005, 2008) demonstrated that a well-tested mesoscale model is suited to simulate air temperature variability in the Phoenix metropolitan region.

The model run was started at 00 Coordinate Universal Time (1700 Local Standard Time, LST). Nested simulations with four domains and resolutions of 27 km (size east-west 3294 km; north-south 2700 km), 9 km (size east-west 1350 km; north-south 1080 km), 3 km (size east-west 594 km; north-south 414 km) and 1 km (size east-west 212 km; north-south 132 km), respectively and 51 vertical layers were performed with WRF. The innermost domain included the Phoenix metropolitan area, surrounding desert and agricultural land. Initial and boundary conditions were provided by the National Center for Environmental Prediction (NCEP) ETA grid 212 (40 km resolution) analysis. Every 6 hours the lateral boundary conditions were updated from the ETA analysis and NCEP/NCAR Reanalysis. Planetary boundary layer processes were included via the non-local closure Medium Range Forecast scheme (Hong and Pan 1996) in the version by Liu et al. (2006).

In order to evaluate the WRF model performance we compared National Weather Service temperature readings for 2 m air temperatures with the simulated data at Phoenix Sky Harbor Airport (Fig. 9.2). Generally the simulations are in close agreement with the measurements, although the simulated temperatures over-predict the peak measured observations for each day of the heat event by about 2°C. A complete agreement between observed and simulated air temperatures cannot be expected because of the complexity of the system, but also because the air temperature recorded at a weather station is a point measurement and is, therefore, conceptually different from the simulated air temperature that is the model grid cell
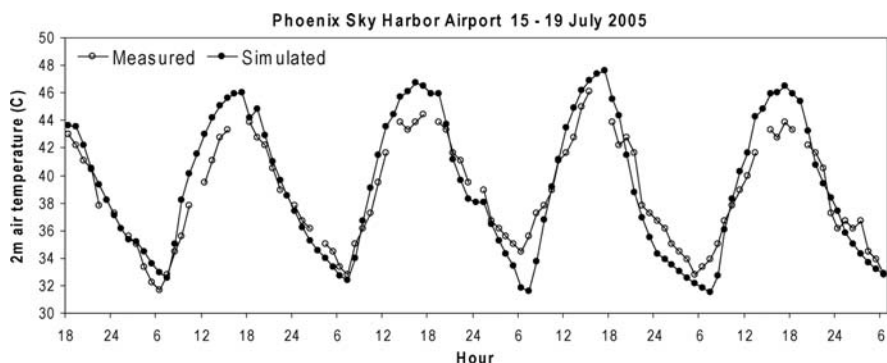

Fig. 9.2 Simulated and measured 2 m air temperature at the National Weather Service station at Sky Harbor Airport in the center of the Phoenix metropolitan region for the time period 15–19 July 2005

average temperature. The two are comparable if the station is placed in an extended homogeneous environment which is rare to find in an urban setting. Other possible reasons for the differences are an inaccurate assessment of the large scale synoptic weather conditions that are influencing the regional simulations through model boundary and initial conditions as provided from a global atmospheric model. These conditions hold true for all sites in the urban area and we assume, therefore, that the model captures differences between neighborhoods satisfactorily.

9.2.5 Land Use/Land Cover Classification System

The 24-category US Geological Survey (USGS) LULC system (Anderson et al. 1976) is the standard input for running WRF. Since the extent and heterogeneity of urban land use of the Phoenix metropolitan area are underrepresented in this dataset (Grossman-Clarke et al. 2005), we chose to use the 2005 12-category LULC classification available for Phoenix at the spatial resolution of 30 m, which is briefly described below.

The general reference LULC classification is based on the expert classification system (Stefanov et al. 2001) originally developed for use with Landsat Thematic Mapper (TM) data to monitor land cover changes in this rapidly expanding urban area. The system performs a posteriori sorting of classes initially derived using the supervised Maximum Likelihood classification. Such reclassification is implemented in the hypothesis-testing framework whereby all initially classified pixels are evaluated using sets of rules and by overlaying with co-registered auxiliary data layers. These layers originate from different sources or are computed directly from a Landsat image and include the county land-use map, image variance texture, water rights database, city boundaries, and Native American reservation boundaries.

The cloud-free Landsat TM image (path 37/row 37) used in the current classification was acquired on March 8, 2005. It was georeferenced and geometrically rectified using high resolution true color aerial photomosaic as a reference source. Raw digital numbers of image bands were converted into true surface reflectance values by applying an atmospheric correction. The final classification has a reported overall accuracy of 83% which is generally acceptable and common for Landsat-derived urban classification level of accuracy. User's accuracy for individual classes varies from 71 to 100% with the exception of commercial/industrial class (51%).

As described in detail in Grossman-Clarke et al. (2005), the derived 12-category LULC map was used to assign land cover class for each WRF 30-second grid cell by using majority rule to determine the highest associated fraction of land cover. We then used the revised land use/cover classifications as input into WRF, and coded the 30-second grid cells as one of the following categories: urban (commercial/industrial); xeric (urban residential draught resistant landscaping); desert (undisturbed natural land); or mesic (urban residential predominantly grass). The categories differed mainly by their type of vegetation and irrigation method (urban and desert – no irrigation; xeric – drought adapted vegetation with drip irrigation; mesic – well watered flood or overhead irrigated). The urban

(commercial/industrial) category was composed entirely of man-made surfaces with no significant vegetation or bare soil, while in the xeric and mesic residential categories, the fractional surface covers were, respectively, man-made (0.73/0.60), vegetation (0.10/0.23), and soil (0.17/0.17). Some peripheral neighborhoods, however, were located in undisturbed desert areas, so we also used the surface characteristics of this fourth classification to drive the model.

9.2.6 Household Survey on Sensitivity to Heat

One way to assess how well WRF simulations relate to human experience is to compare the WRF temperature output to the self-reports of 2006 Phoenix Area Social Survey (PASS) respondents about perceived temperatures and heat-related health problems in the summer of 2005. A comparison of model simulations with residents' reports has not been done before, probably because of the lack of social survey data that spatially corresponds to the model grids. In each of the 40 PASS neighborhoods, described above, 40 randomly selected households were recruited for participation in PASS until a minimum 50% response rate was achieved in each neighborhood. Overall survey response rate was 51% (n = 808). Data from the 2000 Census indicate variable numbers of dwelling units per neighborhood (minimum: 82; maximum: 3833; mean: 888). The percentage of households surveyed per neighborhood also varied from a minimum of 0.6 to a maximum of 24.4, with a mean of 4.4. Surveys were collected using a multi-modal approach (online, telephone, or personal interview), and the respondent who was 18 years or older with the most recent birthday was selected to participate in the study. The survey was administered by the Institute for Social Science Research (ISSR) at Arizona State University from April 29 through September 27, 2006.

As part of PASS, respondents answered the following two questions to gauge their sensitivity to heat: (1) During the summer of 2005, do you think your neighborhood was a lot cooler, a little cooler, a little hotter, or a lot hotter than most other neighborhoods in the Valley or do you think it was about the same temperature as other neighborhoods? (2) During last summer, did you or anyone else in your household have symptoms related to heat or high temperatures such as leg cramps, dry mouth, dizziness, fatigue, fainting, rapid heart beat or hallucinations? (Yes; No).

9.2.7 Neighborhood Demographics

The 2000 US Census Summary Files 1 and 3 for the sample neighborhoods were used to identify the following block group variables for comparisons: population per square mile, median income (US dollars), poverty rate (percent of population below the US government federal poverty guideline), ethnicity (percent minority), and age (median age and ages 65 and older). These variables were used in the analysis to show how different population groups experienced the heat event simulated by WRF.

9.3 Data Analysis

To investigate intra-urban variation in threshold temperatures, the data were analyzed in three phases. The first phase of analysis involved simulating threshold temperatures with the WRF model for the four-day (96 hours) heat event that occurred between July 15 and 19, 2005. Once the temperatures were simulated, GIS was used to map temperature variability for each study site throughout the area and neighborhoods' exposure to extreme heat was quantified. The severity of the heat hazard was calculated by determining the number of exposure hours for each study site to threshold temperatures at or above the 97.5 percentile for the heat event (Fig. 9.3). Exposure to threshold temperatures was then used to create three categories, herein referred to as Heat Intensity Classes. The Heat Intensity Classes were determined by calculating the mean hours of exposure for all 40 neighborhoods and using the difference of one standard deviation to establish each class (Table 9.1). The three levels of heat intensity are: low (less than 9 hours of exposure to temperatures at or above the 97.5 percentile for the 4-day heat event); medium (9–17 hours of exposure); and high (greater than 17 hours).

The final phase of analysis involved comparing the Heat Intensity Classes to household surveys, neighborhood demographics, and LULC types. We analyzed
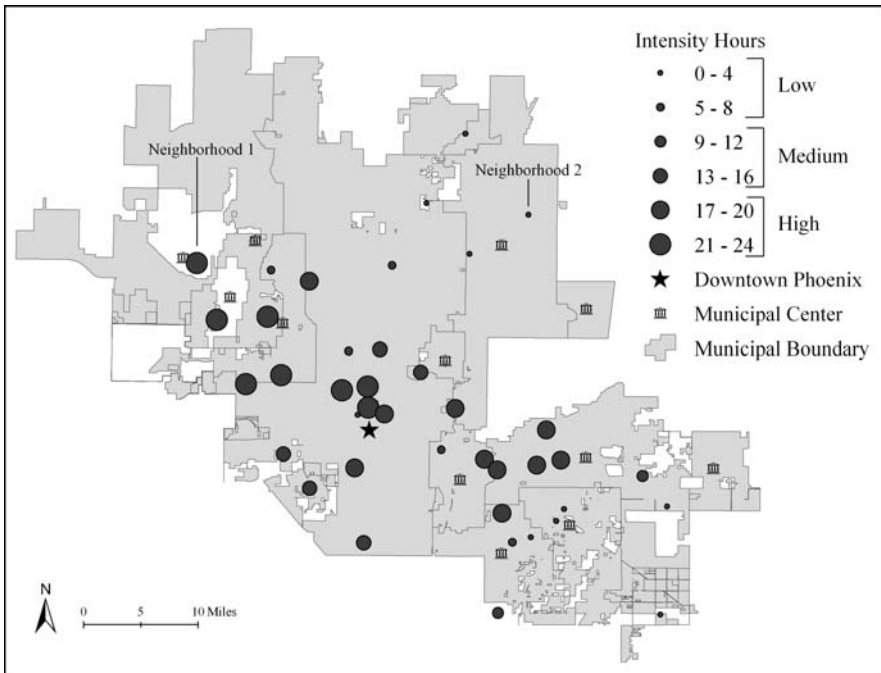

Fig. 9.3 Hours of Exposure to Threshold Temperatures at or above the 97.5 percentile from July 15–19, 2005 by Neighborhood

Table 9.1 Calculation of heat intensity classes based on hours of neighborhood exposure to threshold temperature

Threshold temp	Hours of exposure			Heat intensity classes		
	Range	Mean	SD	Low	Medium	High
97.5 percentile	24	12.6	7.9	<9 hours	9–17 hours	>17 hours

residents' perceptions of and experiences with extreme heat by conducting tests of significance on two measures of heat sensitivity, which serves as a validation of the WRF model. We also examined Census and LULC characteristics by Heat Intensity Class to better understand who is most vulnerable to extreme heat and what role vegetation may play in mitigating neighborhood exposure to threshold temperatures.

9.3.1 Results

9.3.1.1 Distribution of Heat Exposure Time

Tests for spatial autocorrelation presented in Table 9.2 report varying levels of statistical significance. Spatial autocorrelation permits statistical tests (e.g., Moran's *I*, Geary's *c*, Getis-Ord) which investigate spatial patterns by considering the presence of an attribute in space. Tests are based on correlation to neighbors whereby the pattern of a map is such that an area is similar (positive; aggregation) or dissimilar (negative; segregation) to adjacent areas (Burt and Barber 1996). The test both describes the structure of a spatial pattern and is also capable of detecting the presence of directional components (Legendre and Fortin 1989). Moran's *I* analyses on the distribution of simulated temperatures indicate that temperatures are not evenly distributed throughout the study area. While the mean four-day temperature reports modest temperature variation among the 40 neighborhoods (mean: 38.3°C; range: 4.9), hours of exposure to extreme temperatures varies significantly throughout the study area. Exposure to threshold temperatures at or above the 97.5 percentile, for instance, is significantly different among the 40 neighborhoods (mean: 12.6 hours;

Table 9.2 Spatial autocorrelation results for temperature simulations on the 40 neighborhoods

Temperature simulations	Spatial autocorrelation			
	Mean (sd)	Moran's *I*	Z-score	Significance
Mean four-day Temp °C	38.3 (1.1)	0.03	1.73	0.10
Hours exposure: 81st percentile	29.4 (6.1)	0.04	2.37	0.05
Hours exposure: 97.5th percentile	12.6 (7.9)	0.08	3.1	0.01

range: 24). Results, therefore, indicate strong positive spatial patterns where adjacent neighborhoods in some areas are exposed to hazardous temperatures significantly more than other areas.

Figure 9.3 illustrates the varying levels of exposure to threshold temperatures throughout the 40 study sites. The circles represent the number of hours each neighborhood was exposed to threshold temperatures equal to or above the 97.5 percentile. The larger the circles, the greater the exposure to extreme conditions. Generally, the calculations exhibit the UHI pattern where neighborhoods near downtown centers are warmer with higher levels of exposure to threshold temperatures while neighborhoods on the fringe are cooler and have lower levels of exposure to threshold temperatures. However, the pattern of temperature gradients is more complex.

Physical and social processes may help to explain some of the variance in the distribution of air temperatures throughout the study area. Grossman-Clarke et al. (2005), for example, identified strong relationships between temperature and LULC, particularly the abundance of vegetation. In neighborhoods, residential landscapes are managed according to human preferences and availability of resources to cultivate vegetation (Larsen and Harlan 2006; Martin et al. 2004). Additionally, the Phoenix metropolitan region has an elevation gradient with increasing elevation to the north-east which causes differences in air temperature among neighborhoods with comparable land use. Air-flow patterns are influenced by the presence of mountains that typically cause upslope flows during the daytime towards the north and northeast. Downslope flow occurs during the night and is associated with cold advection that reaches various parts of the Phoenix metropolitan area at different times (Brazel et al. 2005). Depending on the location of a neighborhood, cooler or warmer air from areas with different land use/cover in the vicinity might occur. Finally, the current WRF version considers only four urban land use/cover classes and the predominant LULC type is assigned to a model grid cell but might not always be accurately representative, such as for mixed used areas.

Table 9.3 Neighborhood exposure to mean and threshold temperatures (Celsius) by heat intensity class

	Heat intensity class		
Temperature simulations	Low	Medium	High
N neighborhoods	15	10	15
Four-day heat event: Temp °C			
Mean average (sd)	37.2 (1)	38.5 (0.3)	39.2 (0.2)
Mean high (sd)	44.7 (0.9)	45.9 (0.2)	46.5 (0.2)
Mean low (sd)	29.8 (1.2)	30.9 (0.7)	31.8 (0.2)
Four-day heat event: Hours			
81st percentile (sd)	23.8 (6.9)	31.1 (0.9)	33.7 (0.9)
97.5th percentile (sd)	3.3 (2.5)	14.5 (2.6)	20.7 (1.9)

Note: A difference in $1°C = 1.8°F$

Exposure to mean and threshold temperatures by Heat Intensity Class presented in Table 9.3 follow two distinct patterns. When considering mean temperatures (high, low, and average), there is a general positive linear relationship where temperatures increase modestly moving from low to high Heat Intensity Classes. Mean average temperature for the four-day heat event, for instance, increases from 37.2°C (Low) to 38.5°C (Medium) to 39.2°C (High), representing an increase of 2°C from the low to high classes. Exposure to threshold temperatures, however, reflects more pronounced differences among the three intensity classes. On average, neighborhoods in the high Heat Intensity Class were exposed to over six times the number of threshold hours that low intensity neighborhoods experienced during the four-day heat event. Among individual observations, three neighborhoods recorded zero hours of exposure to threshold temperatures in contrast to two neighborhoods that were exposed to twenty-four hours at or above threshold temperatures.

An analysis of the hourly temperature for the four-day heat event confirms variable levels of exposure to threshold temperatures among neighborhoods in the study area. Figure 9.4 presents the average temperature for all neighborhoods in addition to the temperature distribution of two particular neighborhoods. *Neighborhood 1* reported the warmest temperatures of the sample while *Neighborhood 2* reported the coolest temperatures. While the average temperature reached or exceeded the 97.5 percentile (45°C) each day during the heat event, Neighborhood 1 was exposed to considerably higher temperatures in the afternoon as well as the evening and early morning hours. Alternatively, Neighborhood 2 reported significantly cooler temperatures while remaining under 45°C for the duration of the four-day period.
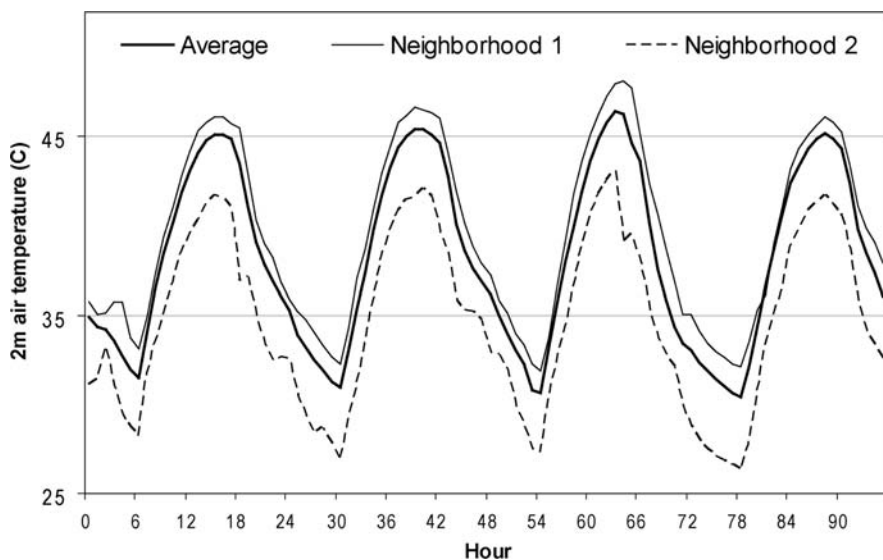

Fig. 9.4 Hourly Neighborhood Temperature (Celsius) Distribution for July 15–19, 2005 (45°C represents the 97.5 percentile)

The 65th hour of the four-day heat event produced the highest simulated temperatures. The temperatures ranged from 46.4°C (Average); 48.2°C (Neighborhood 1); to 43.1°C (Neighborhood 2), representing a difference of 5.1°C (or 9.2°F) between the warmest and coolest neighborhoods in the sample. Hourly neighborhood temperature, therefore, verifies significant variation in levels of exposure to extreme temperatures among the 40 neighborhoods.

9.3.1.2 Perceptions of and Experiences with Extreme Heat

Tests for global spatial autocorrelation analyses indicate the frequency and distribution of two social survey measures for residents' sensitivity to extreme heat are not statistically significant (Table 9.4). In other words, there is not a marked spatial pattern between location and residents' perceptions of and experiences with extreme heat. One explanation for this distribution is the fact that the survey responses reflect the average of 20 unique responses for each location. For instance, *Illness* was determined by coding individual survey responses (No heat-related household illness $= 0$; Yes $= 1$), and then we compared average scores at the neighborhood level. The aggregation of perceptions by neighborhood is subject to many influences which may explain the random distribution of the spatial autocorrelation analyses. In contrast to social perceptions, the 40 neighborhoods are variably exposed to threshold temperatures throughout the study area. In some cases, high intensity neighborhoods are adjacent to low intensity neighborhoods in both the urban core as well as residential suburban areas. Other considerations that could explain the spatial distribution of respondents' views include age and other demographics, housing quality, residential landscaping characteristics, and the availability of other resources that may influence individual residents' perceptions and experiences with extreme heat. Moreover, the question did not ask respondents where the heat incidents occurred, leaving open the possibility that incidents occurred outside their residential neighborhoods.

Analyses of local spatial autocorrelation, however, indicate that perception of risk and illness exhibit spatial clustering in some parts of the study area among adjacent

Table 9.4 Global spatial autocorrelation results for survey responses

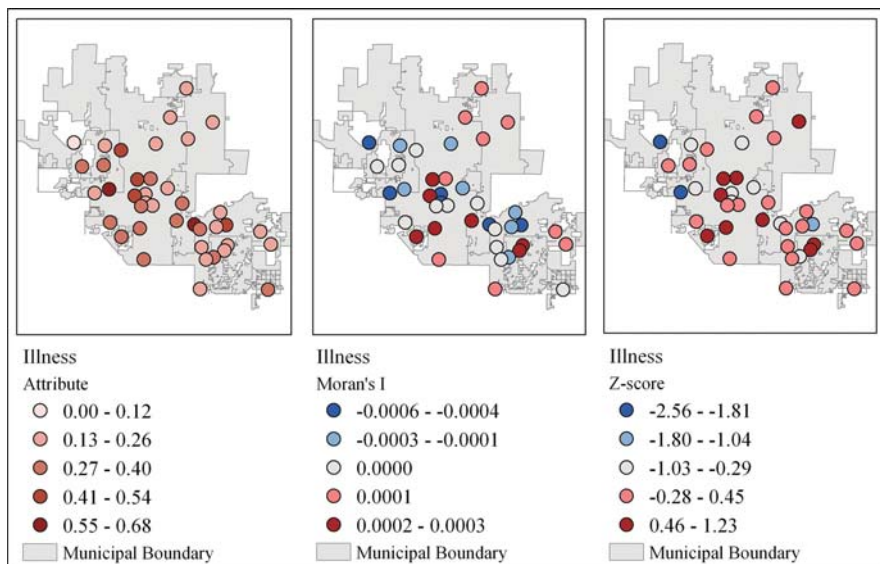| Survey questions	Global spatial autocorrelation		
	Moran's I	Z-score	Significance
Perception of risk			
The temperature of your neighborhood compared to other neighborhoods for summer 2005	−0.05	−0.5	Random
Illness			
Experienced heat-related symptoms in household in summer 2005	−0.04	−0.2	Random

Fig. 9.5 Local spatial autocorrelation results for illness

neighborhoods. Aneslin's Local Index of Spatial Association (LISA) (Anselin 1995) for Moran's *I*, offers empirical insight into a spatial scale by measuring the similarity of an attribute and its spatial configuration to its neighbors. Figure 9.5 , for example, presents three maps illustrating the spatial distribution of self-reported illnesses associated with extreme heat. The first map shows the distribution of the attribute throughout the study area where lower attribute scores reflect fewer heat-related illnesses in the household while higher scores reflect a greater number of heat-related illnesses. The second map shows the distribution of the local Moran's *I* statistic which reports on similarity (low values reflect dissimilar neighbors and high values reflect similar neighbors). The third map presents Z-scores for each neighborhood where the dark red circles represent clustering 'hot spots' of statistically high morbidity (at the 95% confidence level) while the dark blue circles represent clusters of low morbidity. Notice LISA reports significant clustering of illness associated with extreme heat in neighborhoods in Central South Phoenix.

Organized by Heat Intensity Classes, Table 9.5 illustrates differences among residents' perceptions of and experiences with extreme heat. When considering perception of temperature, significantly more respondents in the high Heat Intensity Class reported that the temperature in their neighborhood was "hotter" compared to other Phoenix area neighborhoods for the summer of 2005. Likewise, illness, the second sensitivity measure, shows that almost 31% of respondents in the high Heat Intensity Class reported that someone in their household experienced a heat-related illness for the summer of 2005 in contrast to 24.1% and 24.2% for the low and medium Heat Intensity Classes, respectively. Although the distribution for illness is just outside the 0.10 significance level, results show variation among

Table 9.5 Perceptions of heat stress by heat intensity class

Survey questions	Heat intensity class		
	Low	Medium	High
N Neighborhoods	15	10	15
Perception of temperature			
Temperature in neighborhood compared to others: hotter*	19.0%	22.2%	30.6%
Illness			
Experienced heat-related symptoms: yes	24.1%	24.2%	30.9%

Chi-Square Test (2-sided): *p<0.01
Total number of respondents for Perception of Temperature n = 767; Illness n = 763.

residents' experiences with threshold temperatures. Respondents in high heat intensity neighborhoods, therefore, perceive and experience heat stress more than respondents in neighborhoods of medium and low Heat Intensity Class.

9.3.1.3 Neighborhood Demographics

The first two phases of the analysis found that threshold temperatures and residents' sensitivity to extreme heat are variably distributed throughout the 40 neighborhoods. This phase of analysis explored the types of people who live in the places that are most vulnerable to the exposure of extreme heat. Table 9.6 shows Census block group population characteristics for the following variables: density, income, ethnicity, and age. These variables are all highly related to Heat Intensity Class. Population per square mile, for instance, is roughly twice as high in the high Heat Intensity Class when compared to low and medium intensity classes. Median household

Table 9.6 Population characteristics of neighborhoods by heat intensity class

Demographics	Heat intensity class		
	Low	Medium	High
N neighborhoods	15	10	15
Density			
Population per sq mi	3569	3757	7550
Socioeconomic status			
Household income	$71,903	$62,669	$38,621
% in poverty	5.6	8.3	15.5
Ethnicity			
% minority	20.7	25.9	44.7
Age			
Median age	36.3	40.9	36.6
% ages 65 and over	9.8	20.4	17.5

Source: 2000 US Census, Summary Files 1 and 3

income for the high Heat Intensity Class was just over half the income of the low intensity class, and the percentage of minorities in the high intensity class was more than two times greater than the low class. Interestingly, neighborhoods in the high and medium Heat Intensity Classes had larger percentages of elderly residents, which is cause for concern because the elderly are one of the most vulnerable groups to extreme temperatures. Block groups in low heat intensity neighborhoods are characterized by low population density, higher income, and a relatively low presence of minorities or elderly. We expect that the people in these environments are the least vulnerable to extreme heat because they are likely to have more economic resources to buffer their exposure to threshold temperatures, which are the lowest and of shortest duration in these neighborhoods. Alternatively, high heat intensity class neighborhoods, in general, have high population densities, high percentage of minorities and elderly, and relatively low median household income. We expect that these people have fewer economic resources to buffer their exposure to many more hours of extremely high temperatures. Analyses, therefore, indicate that the urban residents most vulnerable to the risk of heat exposure live in the most hazardous environments.

9.3.1.4 LULC Characteristics

Tables 9.7 and 9.8 present results on the final phase of analysis which examines the relationship between local LULC characteristics, threshold temperatures, and Heat Intensity Classes. Table 9.7 shows that all six neighborhoods classified as urban are located in the high Heat Intensity Class while the eight mesic neighborhoods are all located in the low Heat Intensity Class. Of the 19 xeric neighborhoods, 3 are in the low Heat Intensity Class followed by 7 in the medium and 9 in the high Heat Intensity Class. Table 9.7 is consistent with previous research in showing that land-use patterns and land cover are significant drivers of air temperature differences within the urban area under conditions with weak synoptic forcing (Harlan et al. 2006; Stabler et al. 2005).

There are also some distinct patterns between LULC and simulated temperatures. One particular pattern is a bimodal trend where mesic and desert LULC classes report cooler temperatures when compared to the warmer xeric and urban classes

Table 9.7 Neighborhood LULC categories by heat intensity class

LULC	Heat intensity class		
	Low	Medium	High
N neighborhoods	15	10	15
LULC			
Urban	0	0	6
Xeric	3	7	9
Desert	4	3	0
Mesic	8	0	0

Table 9.8 Neighborhood exposure to threshold temperatures by LULC

	LULC class			
Temperature simulations	Urban	Xeric	Desert	Mesic
N neighborhoods	6	19	7	8
Four-day heat event: Temp ℃				
Mean average (sd)	39.4 (0.2)	38.7 (0.5)	36.9 (1.3)	37.5 (0.6)
Mean high (sd)	46.6 (0.2)	46.0 (0.5)	44.6 (1.3)	44.9 (0.5)
Mean low (sd)	31.8 (0.2)	31.4 (0.4)	29.0 (1.1)	30.3 (0.6)
Four-day heat event: Hours				
81st percentile (sd)	33.8 (0.7)	31.5 (2.8)	22.4 (10)	26.9 (2.3)
97.5th percentile (sd)	21.8 (2.1)	15.8 (5.8)	6.0 (5.8)	4.1 (2.2)

(Table 9.8). The mean high, low, and average temperature of the xeric and urban classes all reported differences in temperature greater than 1°C when compared to mesic and desert classes. The hours at or above threshold temperatures reflect significant differences between the four LULC classes. Neighborhoods in the mesic class, for example, averaged 4.1 hours during the four-day heat event while urban and xeric neighborhoods averaged 21.8 and 15.8 hours at or above threshold temperatures, respectively. These analyses show that urban and xeric neighborhoods are exposed to warmer temperatures for much longer periods of time compared to mesic and desert neighborhoods. Thus, people who live in mesic neighborhoods or near natural desert landscapes have more natural resources in the form of vegetation that helps to lower the ambient temperature and thereby mitigate the impact of heat waves on people.

It is imperative to point out that WRF considers various physical processes in the governing temperature equation to calculate near-surface air temperature. Those physical processes include the strongly land use dependent vertical transport of heat between the atmosphere and the land surface as well as horizontal and vertical advection, horizontal diffusion, net radiative flux convergence and divergence, phase changes of water during fog and cloud formation, adiabatic warming and anthropogenic heating. While a relationship between land use characteristics and air temperature as mediated through vertical turbulent transport of heat can be expected, the strength depends on the synoptic conditions and the time of day and the other physical processes that might dominate temperature tendency near the surface. Using WRF's predecessor, MM5 (Mesoscale Meteorological Model), Grossman-Clarke et al. (2005) investigated the contribution of the different physical processes on the near-surface air temperature under typical summer conditions in Phoenix. Findings indicated that cooling through radiation fluxes accounted for the most significant contribution to changes in air temperature at night and that cooling is enhanced between sunset and midnight by horizontal advection while vertical turbulent transport of heat dominates the temperature tendency for most of the day leading to the reported relationship between land use characteristics and air temperature.

9.4 Discussion

This study offers three contributions to urban hazards and disaster analysis research. Unlike other studies that examine heat-related health disasters for entire cities, this study finds significant intra-urban variability for air temperature, exposure to threshold temperatures, human perceptions, and self-reported illnesses associated with extreme heat. Our first contribution, therefore, is to show that reliance on one climate station as a regional barometer to assess exposure to extreme heat will obscure significant climatic variation within a given urban area and, therefore, the locations and types of individuals who are most at risk from heat hazards.

A second contribution is the development of a methodology for simulating temperature variability for a given study area. Despite some limitations of climate models, which we discussed, we have established a baseline for modeling temperature variability which can be applied to any location. The methodological approach presented in this paper offers the ability to identify high risk urban areas, the areas that will be hit harder, earlier, quicker, and for longer periods of time during an extreme heat event when compared to other places within the same region. Identifying these places helps to enable efforts toward illness prevention and response.

Through the development of this methodology, a third contribution could be the application of this information via a disaster mitigation and response system. The large-scale health disasters caused by recent heat waves have prompted many cities to develop warning systems that alert people to the likely onset of dangerous weather conditions so that adaptive responses are possible. These systems are based on synoptic methods that use local weather data from a central location – such as the city airport – to record relevant variables, relate weather conditions to excess mortality, and create a synoptic analysis that forecasts dangerous heat conditions for a particular city (Kalkstein and Davis 1989; Kalkstein et al. 1996; Sheridan and Kalkstein 2004). While useful for anticipating an upcoming extreme heat event, current systems lack the spatial component reflecting which locations are the most vulnerable. The system developed in our study identifies spatially sensitive degrees of risk to threshold temperatures, based on historical records, to assist disaster efforts prior to a heat event. Benefits of this system are threefold: (1) to inform aid workers where to locate response units prior to the outset of a heat event; (2) to ensure staff and supplies are readily available to aid anyone requiring assistance during a heat event; and (3) to direct policy that may help reduce factors contributing to threshold temperatures (e.g., LULC, building codes) in high risk areas.

9.5 Conclusion

This study employs geospatial methods to investigate extreme heat as a human hazard in the Phoenix metropolitan area. Motivation for this study is to help prevent and reduce heat-induced illnesses, such as heat stroke, exhaustion, dehydration, cardiovascular, and respiratory problems, which strike suddenly and acutely during the warmest times of the year (ICLEI 1998; Semenza et al. 1999). Utilizing both

physical and social data, research findings indicate: (1) Exposure to threshold temperatures is variably distributed among places and people throughout the Phoenix metropolitan area; (2) Residents' perceptions of and experiences with extreme heat parallel simulated air temperatures; (3) The types of people most vulnerable to risk of exposure to extreme temperatures are minorities, elderly, and low income residents. (4) Neighborhoods with mesic landscaping or natural desert surroundings are significantly cooler than neighborhoods with urban or xeric yards. Public expenditures aimed at increasing outdoor amenities (e.g., vegetation, shade, public parks) would provide resources for people to cope during a heat wave event, while helping mitigate human exposure to threshold temperatures.

Simulations from the WRF climate model produced varying levels of mean temperature throughout the Phoenix region in general, and significantly distinct levels of exposure to threshold temperatures across the 40 neighborhoods in particular. While regional atmospheric modeling is currently the best available tool to assess air temperature variability within urban areas, there are limitations to the accuracy of the model output that must be considered when interpreting results. For instance, WRF only employed the predominant neighborhood LULC type as an input variable, which is not always representative in cases of mixed-use areas. Landscape classifications could be further improved in future modeling.

As extreme heat events are expected to increase in intensity, frequency, and duration throughout the world over the next century, monitoring regional weather stations is an insufficient system to mitigate human hazards to heat events. This study illustrates that temperatures vary significantly within the same urban area, and that some residents are at significantly greater risk of exposure to threshold temperatures than others. We applied advanced geotechnical methods to study extreme heat as an urban hazard, the results yielded theoretical, methodological, and practical contributions to disaster analysis research.

References

Anderson, J. R., Hardy, E. E., Roach, J. T., Witmer, R. E., et al. 1976. A Land Use and Cover Classification System for Use with Remote Sensor Data. United States Geological Survey Professional Paper, 964, 36.

Aniello, C., Morgan, K., Busbey, A., Newland, L. et al. 1995. Mapping micro-urban heat islands using Landsat TM and a GIS. *Computer Geosciences*, 21, 965–969.

Anselin, L. 1995. Local Indicators of Spatial Association—LISA. *Geographical Analysis*, 27(2), 93–115.

Arnfield, A. J. 2003. Two decades of urban climate research: a review of turbulence, exchanges of energy and water, and the urban heat island. *International Journal of Climatology*, 23, 1–26.

Braga, A. L. F., Zanobetti, A., Schwartz, J., et al. 2002. The effect of weather on respiratory and cardiovascular deaths in 12 US cities. *Environmental Health Perspectives*, 110, 859–863.

Brazel, A. J., Selover, N., Vose, R., Heisler, G., et al. 2000. A tale of two climates—Baltimore and Phoenix urban LTER sites. *Climate Research*, 15, 123–135.

Brazel, A. J., Fernando H. J. S., Hunt, J. C. R., Selover, N., Hedquist, B. C., Pardviak, E., et al. 2005. Evening transition observations in Phoenix, Arizona. *Journal of Applied Meteorology*, 44(1), 99–112.

Brown, M. 2000. Urban parameterizations for mesoscale meteorological models. In Z. Boybeyi (Ed.), *Mesoscale atmospheric dispersion* (pp. 193–255). Southampton, UK: WIT Press.

Burt, J. E., and Barber, G. M. 1996. *Elementary statistics for geographers*. New York: The Guilford Press.

Census Bureau 2006. 2006 American Community Survey. www.census.gov; accessed October 26, 2008.

(CDC) Centers for Disease Control and Prevention 2005. Heat-related mortality – Arizona,1993–2002 and United States, 1979–2002. *Morbidity & Mortality Weekly Report*, 54 (25):628–630.

(CDC) Centers for Disease Control and Prevention 2006. Extreme heat: a prevention guide to promote your health and safety. http://www.bt.cdc.gov/disasters/extremeheat/heat_guide.asp; accessed 4/29/08.

Choi, G. Y., Choi, J. N., Kwon, H. J., et al. 2005. The impact of high apparent temperature on the increase of summertime disease-related mortality in Seoul: 1991–2000. *Journal of Preventive Medicine and Public Health*, 38, 283–290.

Civerolo, K. L., Sistla, G., Rao, S. T., Nowak, D. J., et al. 2000. The effects of land cover in meteorological modeling: implications for assessment of future air quality scenarios. *Atmospheric Environment*, 34, 1615–1621.

Confalonieri, U., Menne, B., Akhtar, R., Ebi, K. L., Hauengue, R. S., Kovate, B., Woodward, A., et al. 2007. Human Health. In M. L. Parry, O. F. Canziani, J. P. Palutikof, P. J. van der Linden and C. E. Hanson (Eds), *Climate Change 2007: Impacts, Adaptation and Vulnerability*. Contribution of Working Group II to the Fourth Assessment Report of the Intergovernmental Panel on Climate Change. Cambridge, UK: Cambridge University Press.

Curriero, F. C., Heiner, K. S., Samet, J. M., Zeger, S. L., Strug, L., Patz, J. A., et al. 2002. Temperature and mortality in 11 Cities of the eastern United States. *American Journal of Epidemiology*, 155, 80–87.

DeGaetano, A. T. and Allen, R. J. 2002. Trends in twentieth-century temperature extremes across the United States. *Journal of Climate*, 115, 3188–3205.

Grimm, N. B. and Redman, C. L. 2004. Approaches to the study of urban ecosystems: the case of Central Arizona – Phoenix. *Urban Ecosystems*, 7, 199–213.

Grimmond, C. S. B. 2005. Progress in measuring and observing the urban atmosphere. *Theoretical and Applied Climatology*. doi: 10.1007/s00704-00005-00140-00705.

Grossman-Clarke, S., Zehnder, J. A., Stefanov, W. L., Liu, Y., Zoldak, M. A. 2005. Urban modifications in a mesoscale meteorological model and the effects on near surface variables in an arid metropolitan region. *Journal of Applied Meteorology*, 44, 1281–1297.

Grossman-Clarke, S., Liu, Y., Zehnder, J. A., Fast, J. D., et al. 2008. Simulation of the Urban Planetary Boundary Layer in an arid metropolitan Area. *Journal of Applied Meteorology and Climatology*, 47(3), 752–768.

Harlan, S. L., Brazel, A. J., Prashad, L., Stefanov, W. L., Larsen, L., et al. 2006. Neighborhood microclimates and vulnerability to heat stress. *Social Science & Medicine*, 63, 2847–2863.

Harlan, S. L., Budruk, M., Gustafson, A., Larson, K., Ruddell, D., Smith, V. K., Yabiku, S. T., Wutich, A., et al. 2007. Phoenix Area Social Survey 2006 Highlights: Community and Environment in a Desert Metropolis. Central Arizona – Phoenix Long-Term Ecological Research Project, Contribution No. 4. Global Institute of Sustainability, Arizona State University.

Harlan, S. L., Brazel, A. J., Jenerette, G. D., Larsen, L., Jones, N. S., Prashad, L., Stefanov, W. L., et al. 2008. Made in the shade: The inequitable distribution of the urban heat island. *Research in Social Problems and Public Policy*, 15, 173–202.

Hedquist, B. C., and Brazel, A. J. 2004. Urban heat island (UHI) measures for the S.E. metropolitan area of the CAP LTER: transects versus fixed stations. Presented at the 6th Annual CAP LTER Poster Symposium, Tempe, AZ.

Hong, S. Y., and Pan, H. L. 1996. Nonlocal boundary layer vertical diffusion in a medium-range forecast model. *Monthly Weather Review*, 124, 2322–2339.

(ICLEI) International Council for Local Environmental Initiatives 1998. Cities at risk: assessing the vulnerability of United States cities to climate change. Toronto, Canada.

(IPCC) Intergovernmental Panel on Climate Change 2007. Climate Change 2007: Synthesis Report. http://www.ipcc.ch/pdf/assessment-report/ar4/syr/ar4_syr.pdf; accessed 4/29/08.

Jenerette, G. D., Harlan, S. L., Brazel, A. J., Jones, N., Larsen, L., Stefanov, W. L., et al. 2007. Regional relationships between vegetation, surface temperature, and human settlement in a rapidly urbanizing ecosystem. *Landscape Ecology*, 22, 353–365.

Kalkstein, L. S., and Davis, R. E. 1989. Weather and human mortality: an evaluation of demographic and inter-regional responses in the United States. *Annals of the Association of American Geographers*, 79, 44–64.

Kalkstein, L. S., and Greene, J. 1997. An evaluation of climate/mortality relationships in large US cities and the possible impact of a climate change. *Environmental Health Perspectives*, 105(1), 84–93.

Kalkstein, L. S., Jamason, P. P., Greene, J. S., Libby, J. Robinson, L., et al. 1996. The Philadelphia hot weather-health watch warning system: development and application, summer 1995. *Bulletin of the American Meteorological Society*, 77, 1519–1528.

Kilbourne, E. M. 2002. Heat-related illness: current status of prevention efforts. *American Journal of Preventive Medicine*, 22, 328–329.

Klinenberg, E. 2002. *Heat wave: A social autopsy of disaster in Chicago*. Chicago: University of Chicago Press.

Kusaka, H., and Kimura, F. 2004. Coupling a single-layer urban canopy model with a simple atmospheric model: impact on urban heat island simulation for an idealized case. *Journal of the Meteorological Society of Japan*, 82, 67–80.

Larsen, L., and Harlan, S. L. 2006. Desert dreamscapes: residential landscape preference and behavior. *Landscape and Urban Planning*, 78, 85–100.

Larson, J. 2006. Setting the record straight: more than 52,000 Europeans died from heat in summer 2003. *Earth Policy Institute*. Available at: http://www.earth-policy.org/Updates/2006/Update56.htm. Accessed October 19, 2007.

Legendre, P., and Fortin, M. J. F. 1989. Spatial pattern and ecological analysis. *Vegetation*, 80, 107–138.

Lin, C.-Y., Chen, F., Huang, J. C., Chen, W-C., Liou, Y.-A., Chen, W.-N., Liu, S-C., et al. 2008. Urban heat island effect and its impact on boundary layer development and land-sea circulation over northern Taiwan. *Atmospheric Environment*, 42, 5635–5649.

Liu, Y., Chen, F., Warner, T., Basara, J., et al. 2006. Verification of a Mesoscale Data-Assimilation and Forecasting System for the Oklahoma City Area During the Joint Urban 2003 Field Project. *Journal of Applied Meteorology*, 45, 912–929.

Lowry, W. 1967. The climate of cities. *Scientific American*, 217, 15–23.

Martilli, A. 2007. Current research and future challenges in urban mesoscale modeling. *International Journal of Climatology*, 27(14), 1909–1918.

Martin, C. A., Warren, P. S., Kinzig, A. P., et al. 2004. Neighborhood socioeconomic status is a useful predictor of perennial landscape vegetation in residential neighborhoods and embedded small parks of Phoenix, Arizona. *Landscape and Urban Planning*, 69, 355–368.

Masson, V. 2006. Urban surface modeling and the meso-scale impact of cities. *Theoretical and Applied Climatology*, 84(1), 35–45.

McGeehin, M. and Mirabelli, M. C. 2001. The potential impacts of climate variability and changer on temperature-related morbidity and mortality in the United States. *Environmental Health Perspectives*, 109, 185–189.

McMichael, A. J., Woodruff, R. E., Hales, S., et al. 2006. Climate change and human health: present and future risks. *Lancet*, 367, 859–869.

Meehl, G. A., and Tebaldi, C. 2004. More intense, more frequent, and longer lasting heat waves in the 21st century. *Science*, 305, 994–997.

Michelozzi, P., DeSario, M., Accetta, G., De'Donato, F., Kirchmayer, U., D'Ovidio, M., Perucci, C., et al. 2006. Temperature and summer mortality: geographical and temporal variations in four Italian cities. *Journal of Epidemiology and Community Health*, 60, 417–423.

Naughton, M. P., Henderson, A., Mirabelli, M. C. et al. 2002. Heat-related mortality during a 1999 heat wave in Chicago. *American Journal of Preventive Medicine*, 22, 221–227.

Oke, T. R. 1982. The energetic basis of the urban heat island. *Quarterly Journal of the Royal Meteorological Society*, 108, 1–24.

Oke, T. R. 1997. Part 4: The changing climatic environments: urban climates and global environmental change. In R. D. Thompson and A. Perry (eds.), *Applied Climatology Principals and Practice* (pp. 273–287). London: Routledge.

O'Neill, M. S., Jarrett, M., Kawachi, I., Levy, J. I., Cohen, A. J., Gouveia, N., Wilkinson, P., Fletcher, T., Cifuentes, L., Schwartz, J., et al. 2003. Health, wealth, and air pollution: advancing theory and methods. *Environmental Health Perspectives*, 111, 1861–1870.

Patz, J. 2005. Guest editorial: satellite remote sensing can improve chances of achieving sustainable health. *Environmental Health Perspectives*, 113, A84–85.

Patz, J., Campbell-Lendrum, D., Holloway, T., Foley, J. A., et al. 2005. Impact of regional climate change on human health. *Nature*, 438, 310–317.

Seaman, N. L. 2000. Meteorological modeling for air-quality assessments. *Atmospheric Environment*, 34, 2231–2259.

Semenza, J. C., Rubin, C. H., Falter, K. H., Selanikio, J. D., Flanders, W. D., How, H. L., Wilhelm, J. L., et al. 1996. Heat-related deaths during the July 1995 heat wave in Chicago. *American Journal of Preventive Medicine*, 16(4), 269–277.

Semenza, J. C., McCullough, J. E., Flanders, W. D., McGeehin, M., Lumpkin, J. R. et al. 1999. Excess hospital admissions during the July 1995 heat wave in Chicago. *American Journal of Preventive Medicine*, 16(4), 269–277.

Shamrock, W. C., Klemp, J. B., Dudhia, J., Gill, D. O., Barker, D. M., Wang, W., Powers, J. G., et al. 2005. A Description of the Advanced Research WRF Version 2. NCAR Technical Note.

Sheridan, S. C. and Kalkstein, L. S. 2004. Progress in heat watch-warning system technology. *Bulletin of the American Meteorological Society*, 85, 1931–1941.

Smoyer-Tomic, K. E., and Rainham, D. G. C. 2001. Beating the heat: Development and evaluation of a Canadian hot weather health-response plan. *Environmental Health Perspectives*, 109, 1241–1248.

Smoyer, K. E., Rainham, D. G., Hewko, J. N., et al. 2000. Heat-related stress mortality in five cities in southern Ontario: 1980–1996. *Institutional Journal of Meteorology*, 44(1809), 190–197.

Stabler, L. B., Martin, C. A., Brazel, A. J., et al. 2005. Microclimates in a desert city were related to land use and vegetation index. *Urban Forestry and Urban Greening*, 3, 137–147.

Stefanov, W. L., Ramsey, M. S., Christensen, P. R., et al. 2001. Monitoring urban land cover change: an expert system approach to land cover classification of semiarid to arid urban centers. *Remote Sensing of Environment,* 77, 173–185.

Taha, H. 1997a. Modeling the impacts of large scale albedo changes on ozone air quality in the south coast air basin. *Atmospheric Environment*, 31, 1667–1676.

Taha, H. 1997b. Urban climates and heat islands: albedo, evapotranspiration, and anthropogenic heat. *Energy and Buildings, 25*, 99–103.

Voogt, J. A. 2002. Urban Heat Island. In I. Douglas (ed.), *Encyclopedia of global environmental change* (pp. 660–666). Chichester: John Wiley and Sons.

Voogt, J. A., and Oke, T. R. 2003. Thermal remote sensing of urban climates. *Remote Sensing of Environment*, 86, 284–370.